DOI: 10.5327/Z2317-4889201400030003

ARTICLE

Aeromagnetic and physical-chemical properties of some complexes from Goiás Alkaline Province

Dados aeromagnéticos e Propriedades físico-químicas de alguns complexos da Província Alcalina de Goiás

Alanna C. Dutra[1]*, Yára R. Marangoni[2], Ricardo I. F. Trindade[2]

ABSTRACT: The Goiás Alkaline Province (GAP), located on the north edge of the Paraná Basin, has alkaline complexes with strong magnetic signatures. The 3D inversion of magnetic signal was performed on the aeromagnetic data. Since the intrusions present a strong remnant magnetization, as measured in the laboratory, a careful analysis of this component was also realized. The sum vector of the remnant and induced components were used as a virtual induced magnetic field during the 3D inversion process. The geometric parameters were obtained from the quantitative analysis of magnetic data, using Total Gradient Direction and Analytical Signal Phase, performed over magnetic signal reduced to the pole. Magnetic susceptibility and density were measured in laboratory. All this information were used as the initial model in the inversion. The results of 3D inversion show that the alkaline intrusions have roots up to 10-12 km depth. The magnetic susceptibility is distributed in almost spherical and cylindrical shapes. The possibility of spherical shapes arise the hypothesis that the GAP intrusions at the northern part of the province represent magmatic chambers. The alkaline magma ascends from the lithosphere, and used two main fault systems as space for emplacement. These faults systems appear in the magnetic signal analysis as linear magnetic features. Chemical analysis confirmed the alkaline and subalkaline character of the magmas. The high MgO content shows the primitive character of these intrusions but the Ba anomaly indicates a possible crustal contamination.

KEYWORDS: Alkaline magmatism; magnetic data; remnant magnetization; 3D inversion.

RESUMO: *A Província Alcalina de Goiás (PAGO), localizada na borda norte da Bacia do Paraná, tem complexos alcalinos com fortes assinaturas magnéticas. A inversão do sinal 3D magnética foi realizada nos dados de magnetometria. Amostras coletadas em campo de algumas dessas intrusões alcalinas apresentam forte magnetização remanescente, como mostram as medidas tomadas em laboratório, assim, uma análise cuidadosa desta componente também foi realizada. O vetor soma dos componentes remanescente mais induzidas foram usadas como um campo magnético induzido virtual durante o processo de inversão 3D dos dados magnéticos. Os parâmetros geométricos foram obtidos a partir da análise quantitativa de dados magnéticos, usando Gradiente Horizontal Total e Fase dos Sinal Analítico. As Susceptibilidades magnéticas e densidades foram medidas em laboratório. Todas as informações foram utilizadas como modelo inicial para a inversão. Os resultados da inversão 3D mostram que as intrusões alcalinas têm raízes até 10-12 km de profundidade. A susceptibilidade magnética é distribuída em formas quase esféricas e cilíndricas. A possibilidade das formas esféricas ocorre da hipótese de que as intrusões da GAP na parte norte da província representam câmaras magmáticas. O magma alcalino ascendeu da litosfera e usou dois principais sistemas de falhas como caminho preferencial para sua colocação. Estes sistemas de falhas aparecem na análise do sinal magnético como feições magnéticas lineares. A análise química confirmou o caráter alcalino e subalcalino dos magmas. O alto teor de MgO mostra o caráter primitivo dessas intrusões, mas a anomalia Ba indica uma possível contaminação crustal.*

PALAVRAS-CHAVE: *Magmatismo alcalino; dados magnéticos; magnetização remanescente; inversão 3D.*

[1]Department of Physics of the Earth and Environment, Institute of Physics, Universidade Federal da Bahia – UFBA, Salvador (BA), Brasil. *E-mail: alannacd@ufba.br*

[2]Department of Geophysics, Institute of Astronomy, Geophysics and Atmospheric Sciences, Universidade de São Paulo – USP, São Paulo (SP), Brasil. *E-mail: yara@iag.usp.br; rtrindad@iag.usp.br*

*Corresponding author

Manuscrito ID 30043. **Recebido em:** 07/10/2013. **Aprovado em:** 09/06/2014.

INTRODUCTION

The North border of the Paraná Basin, in Central Brazil, is characterized by an erosive scenario very active during the Upper Cretaceous with the intrusion of alkaline magmatism in the area. Three provinces are found, Goiás Alkaline Province, Alto Paranaíba Igneous Province and Porixoréu Province. This magmatism is set in groups of intrusions in Goiás, Minas Gerais and Mato Grosso states, some hundreds of kilometers apart. The intrusions are disposed in linear arrangements parallel or with different angles in relation with the basin border, sometimes inside the basin and sometimes just outside it. The provinces shows similarities and differences in the magma type, some of the intrusions have carbonatites, but share a very similar geophysical signature: high Bouguer anomalies and strong magnetic signal.

The Goiás Alkaline Province (GAP) is located in Goiás State, at the Paraná Basin border and in terrains of Bom Jardim de Goiás Volcanic Arc and other Precambrian terrains, it occupies an area of 250 x 70 km. The province presents different magma sets: the north part is characterized by alkaline mafic ultramafic intrusions, sub volcanic alkaline intrusions at the central portion and volcanic flows in the south part (Fig. 1). The alkaline complexes of the north region are intrusive and present different sizes. The main lithotypes found in the intrusions are dunites, peridotites, diverse pyroxenites, gabbro, alkali-gabbro, nepheline syenite and fenitization products. At the central and south portions it is easy to found dikes, sills and lava flows disposed in a linear band at the NW-SE direction. These structures might take advantage of faults in that direction during their emplacement (Junqueira-Brod *et al.* 2002). The intrusive alkalines at the north part are the Morro do Engenho, Santa Fé, Montes Claros de Goiás, Arenópolis, Buriti, Córrego dos Bois e Morro do Macaco. The subvolcanics at the central part and lava flows at south are the Amorinópolis, Águas Emendadas and Santo Antônio da Barra. All of them are numbered in the map of Fig. 1.

The Precambrian terrains that host part of the GAP is composed of volcano-sedimentary sequences, granites and orthogneiss, post tectonic intrusions of diorite gabbro and granite. The orthogneiss are mainly granite and granodiorite calco alkaline with high K, they show very restrict tonalites facies. The most NW intrusions cut Furnas Formation from Paraná Basin. This formation is of coarse sandstones of Devonian.

The GAP intrusions have a strong magnetic and gravimetric signal. They are so characteristic that some anomalies that have no related outcrop have been inferred as signal of subsurface intrusive. The lithology of the mafic intrusive are appropriate for the strong geophysical signal because of the comparatively high density and magnetite content compared with the surrounding geology. The magnetic signal was used to infer the distribution of magnetic susceptibility in depth and constrain possible geometry for the intrusives. The choice method of study was the 3D inversion constrained by results of application of Analytical Signal Phase and Horizontal Total Gradient. A careful analysis of magnetic properties was also made to determine possible remnant magnetization component.

The magnetic inversion may not be possible if the magnetic signal carries a remnant component. The remnant magnetization can change the interpretation of the geological source since it influence the magnetic anomaly. The effects of this component have been studied in detail by Brooks (1962) and Roest and Pilkington (1993), among others. The problem appears when the total magnetization direction is unknown and different from the induced field at the survey time. The possibility to overcome this common situation is to determine the remnant component in a laboratory and to work with the sum of the induced and remnant. In this work the sum vector was considered the virtual field direction, in the sense that it substitutes the induced field. The results obtained in the inversion proved that this is a feasible way to work with magnetic data when remnant magnetization is present.

PHYSICAL-CHEMICAL ANALYSIS RESULTS

84 samples were collected from 8 sites in the studied region, all of them marked in Figure 1. Density (g/cm^3) and magnetic susceptibility (SI) are shown in Figure 2. The mean density value was 2.71 g/cm^3, a value lower than expected for the samples lithology. The mean magnetic susceptibility was 0.02 (SI). Samples dunite (01) and syeno-diorite (09A) show strong weathering and are altered, that may be responsible for the low density values observed. These values were considered despite the low density values because the samples show good results as the values of magnetization and magnetic susceptibility, and has been verified by optical microscope that the magnetic minerals are well preserved in the samples. Despite this alteration the magnetic property is preserved, since they have high iron and magnesium oxides content as geochemical analysis confirmed.

Occurrences of Cretaceous alkaline rocks have been described with focus on the petrochemistry and mineral chemistry (Sgarbi 1998, Lacerda *et al.* 2000, Brod *et al.* 2005, Comin-Chiaramonti & Gomes 2005). In this study the chemical analysis of collected samples confirmed the ultrabasic-alkaline nature of the samples with 41% < SiO_2 < 44%, namely

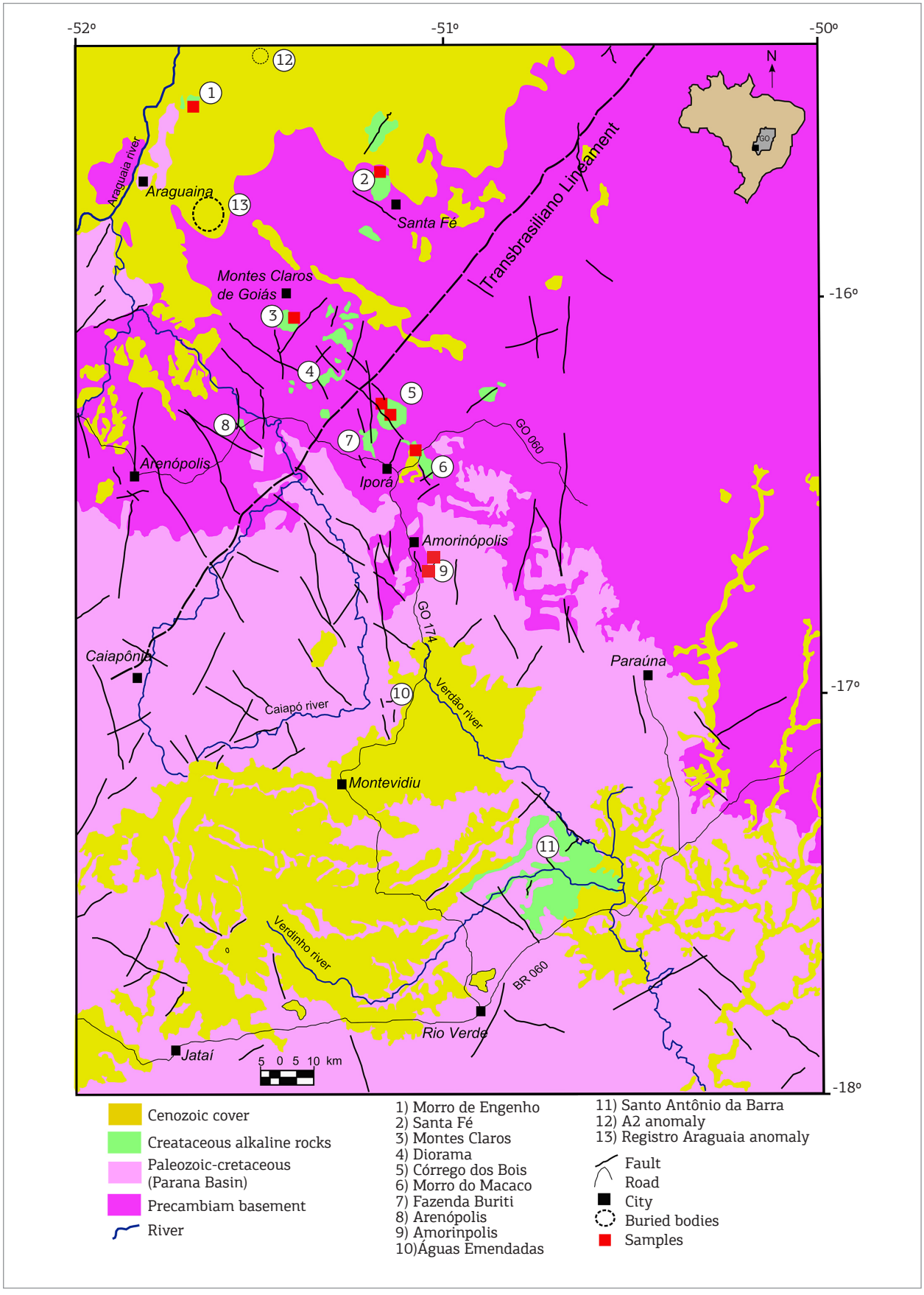

Figure 1. Geological map of Goiás Alkaline Province (Brod *et al.* 2005).

gabbro and ijolite. Among the studied rocks it is possible to found basic rocks (45% < SiO_2 < 52%), gabbro and syenite diorite, and intermediate rocks (53% < SiO_2 < 57%), alkaline granite and granodiorite. The basic and ultrabasic samples has high contents of CaO (2.18 to 16.3 wt %) and TiO_2 (2.44 to 4.7 wt %). The MgO content (3.83 and 39.25%) shows the primitive character of these intrusions, with values of 0.11 to 0.75 for the MgO/MgO+FeO ratio (FeOt between 3.22 and 13.47%). The chemical results are in Table 1.

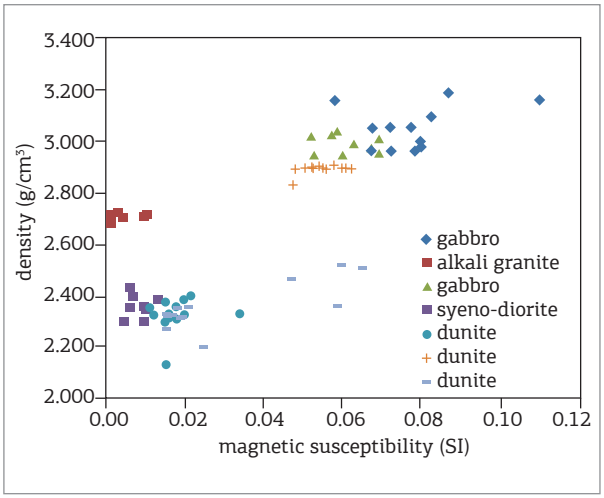

Figure 2. Plot of density (g/cm³) and magnetic susceptibility (SI) of GAP samples.

Figure 3 shows de result from chemical analysis in a TAS diagram with alkaline and sub-alkaline rocks fields defined by Cox *et al.* (1979). In the same figure are the results from previous work at the GAP made by Junqueira-Brod *et al.* (2005), grey circles. It is possible to see that the collected samples present similarities with previous works.

Some samples present high concentration of Ni (> 100 ppm) and Cr (> 1000 ppm) that coexist with high concentration of lithophile elements, like Zr (between 43.9 – 436.3 ppm), Sr (between 175.7 – 1139.9 ppm), Ba (between 59.2 – 3500.8 ppm). The Ba anomaly is a strong characteristic of a variety of intracontinental magmatism and can be attributed to the phlogopite presence in the mantle source or crustal contamination. The fractioning of light rare earth elements (REE) can be interpreted as a result of high content of clinopyroxene and phlogopite in the melts. The high content of Cr (120 – 6660.6 ppm) and Ni (336 – 9251.4 ppm) are consistent with the ultramafic composition of the samples; particularly Ba, Sr and REE's sum go to a few decimals of one percent. Nb (5 – 123 ppm) and Zr (44 – 436 ppm) concentrations are relatively high.

AEROMAGNETIC DATA

A new data set of aerogeophysical survey, magnetic and radiometric data, is available for Goiás State, Central Brazil.

Table 1. Chemical analysis results from major (%) and trace (ppm) elements. Measurements were done with Spectrometry X-Ray Fluorescence using melted matrix of borate. Trace elements were analyzed in pressed samples.

Sample	01	06	09A	09B	09C	10A	10B
SiO_2	45.00	46.15	51.48	68.29	47.20	43.15	39.43
TiO_2	0.13	1.61	2.44	0.58	3.43	3.97	4.70
Al_2O_3	0.51	16.96	15.40	14.29	14.29	7.41	9.58
Fe_2O_3t	14.56	12.80	10.77	5.39	11.17	13.88	14.97
MnO	0.18	0.19	0.18	0.11	0.20	0.22	0.23
MgO	38.25	7.80	4.25	0.61	3.83	13.23	11.77
CaO	0.03	11.73	7.14	2.18	9.81	16.03	13.19
Na_2O	0.21	2.36	3.63	3.47	2.14	0.88	2.83
K_2O	0.11	0.23	4.09	4.90	7.16	0.66	2.50
P_2O_5	0.01	0.17	0.61	0.17	0.79	0.57	0.82
Cr	6660.0	196.7	114.6	145.7	28.8	1854.9	453.0
Ni	9251.4	91.5	19.0	8.1	8.6	336.0	146.6
Ba	86.9	56.2	1046.8	965.8	840.5	3500.8	1308.5
Rb	23.1	5.5	81.9	165.5	47.4	100.3	66.8
Sr	--	440.9	870.5	176.2	619.7	343.8	1139.9
La	--	3.6	79.3	66.5	62.6	44.3	73.7
Ce	203.7	16.8	78.6	88.6	--	256.3	110.4
Zr	43.9	103.2	392.9	436.3	297.4	195.8	279.8
Y	57.8	30.0	32.0	36.9	32.3	10.5	20.3
Nb	0.68	4.6	77.6	17.8	123.4	--	94.1
Cu	--	54.5	8.5	10.8	5.4	28.7	54.8
Zn	105.6	115.8	92.8	96.8	93.0	44.3	90.2

Most of the GAP region has been surveyed in 2004 at the first stage of the project. The area was flown at a height of 100 m, with line 0.5 km apart at the NS direction with ten measurements at 0.1 s interval. Control lines were in the EW direction 5 km apart. Survey was positioned with GPS precision better than 10 m (LASA 2004). The used parameters imply that anomalies with spatial dimensions less than 1 km (twice the interval of sample profile) can not be well represented (Telford *et al.* 1990, Blakely 1996). Data processing included corrections for diurnal variation, parallax error, leveling and microleveling of profiles and removal of IGRF calculated at flight height referred to year 2000 and at the date of August 2004. The final available product is the total field magnetic anomaly (as shown in Fig. 4). Details of all the stages involved in the aeromagnetic survey and field data treatment can be found in the survey rapport (LASA 2004).

The interpolation method used was bidirectional, with the grid spacing of 125 x 125 m^2. The line direction is very close to either north-south, this approach will also enhance geological trends perpendicular to the line direction. Since we ideally want to enhance features perpendicular to the survey line direction, we should specify this angle to be perpendicular to the line direction.

In Fig. 4 the GAP intrusions show a strong magnetic anomaly. It is remarkable the coincidence between the two geophysical signals and the high amplitude that they have for most of the outcrops. Both signals display anomalies almost circular over the GAP intrusions. Magnetic anomalies have diameters in the order of 10 km and lineaments are longer than 20 km indicating that both type of structures referred to intrusions with considerable size located at the upper and medium crust. The expected aliasing effect because of the distance between plane and intrusions top is about 20% (Reid 1980) since most part of the intrusions are exposed. This effect may be considerable and some part of the signal could be lost, but as the anomalies are extensive and have been surveyed by a few flight lines (5 or more) it is reasonable to consider that the map of Fig. 4 shows a good relationship with the geological situation in the area.

The quantitative analysis of the magnetic data was performed in the frequency domain. To avoid border effects the grid was enlarged at their borders by 10% with values extrapolated from the original grid. Frequencies above Nyquist number, 1.9 cycle/km in the area, were eliminated since they may represent noise.

It was calculated the Total Horizontal Gradient (THG) and Analytical Signal Phase (ASP) of the total anomaly magnetic field. Applications of these two techniques help to infer geometry and size of the magnetic fonts. The work

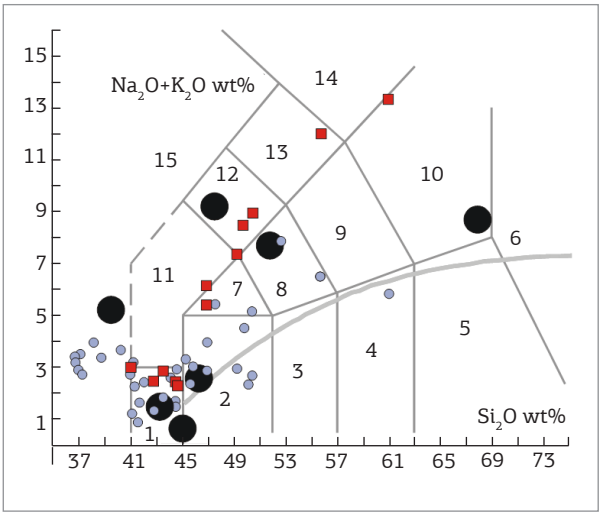

Figure 3. Diagram of SiO^2 versus (N^2O + K^2O (TAS: Le Maitre 1989, Le Bas et al. 1986). The gray line divides the sub-alkaline series from the alkaline series (high alkalies). Black circles, this work; grey circles, after Junqueira-Brod et al. 2005; red squares, after Brod et al. 2005. Nomenclature (in parethesis the intrusive equivalent): 1, picrobasalt (ultramafite); 2, basalt (gabbro); 3, basaltic andesite (diorite); 4, andesite (Qz-diorite); 5, dacite (granodiorite); 6, rhyolite (granite); 7, trachybasalt (monzogabbro); 8, basaltic trachyandesite (monzodiorite); 9, trachyandesite (monzonite); 10, trachyte, if quartz < 20% (Qz-monzonite), trachydacite if quartz > 20% (syenite); 11, tephrite if olivine < 10% (foid bearing monzogabbro), basanite if olivine > 10% (foid bearing gabbro); 12, phonotephrite (foid bearing monzodiorite); 13, tephrifonolite (foid bearing monzosyenite); 14, phonolite (foid syenite); 15, foidite (foidolite).

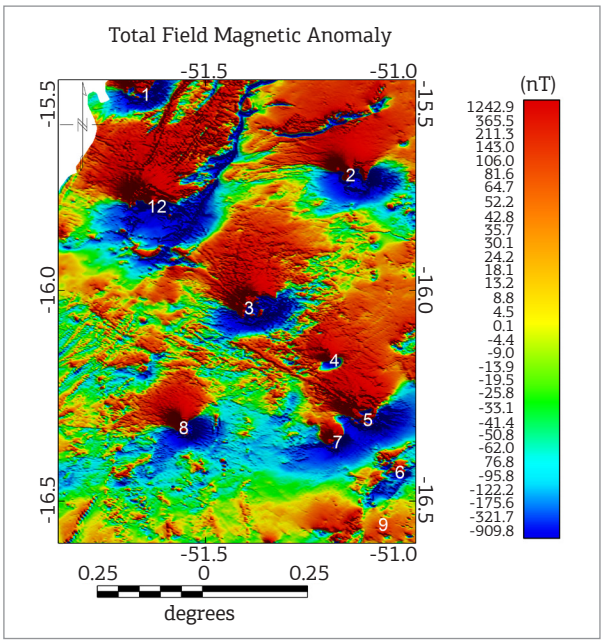

Figure 4. Total field magnetic anomaly. Numbers refer to alkaline location as in Figure 1.

hypothesis is that the peaks of the signal amplitude are originated by vertical contacts and, in this case, the anomaly width is proportional to its depth. The results obtained are show in Fig. 5. The THG and ASP were performed over the total magnetic anomaly reduced to the pole. In Fig. 5 it is possible to notice that each anomaly results from an isolated intrusion (or body when there is not an outcrop), the limits are marked and results in almost circular shape. Magnetic lineaments were also enhanced and are mostly in the NW-SE direction except close to anomaly 12 (Registro do Araguaia) where a striking NE-SW lineament marks the north part of the inferred intrusion and extends behind the limits of the area. This region is totally recovered by quaternary sediments from the Araguaia River. It is interesting to note that the NW-SE features cross some of the anomalies but does not deform it, as can be seen in the anomalies 3 (Montes Claros) and 5 (Córrego dos Bois). Some of these lineaments also show relation with mapped faults in the area.

The alkaline provinces show a clear tectonic control of magmatism by crustal discontinuities mainly extensional or wrenching fault zones (magnetic lineaments) along the present-day borders of sedimentary basins (magnetic signal with smoothed relief). Inheritance of Proterozoic crustal discontinuities have played a major role on the alkaline magmatism. Changes in the stress-fields and reactivations of regional structures in different pulses produced a great range of structural weakness along which alkaline magmas were emplaced or reached the surface. These tectonic controls explain the regional distribution of alkaline magmatism in the central-southeastern region of the Brazilian Platform.

MAGNETIC PROPERTIES

GAP intrusion show a strong magnetic anomaly composed of induced (M_i) and remnant (M_R) magnetization, as has been already discussed by Dutra and Marangoni (2009). Since the remnant magnetization is very strong it was necessary to collect oriented samples and to determine their remnant magnetic properties. Figure 8 shows a plot of the magnetization components. In this Figure it is possible to observe that almost all of them have Konigsberger ration (Q) greater than one and just a few have Q = 1, that emphasizes the importance of the remnant component.

In order to determine remnant magnetization direction, measurements were done on 84 cylinders of oriented field samples collected in the area (location of site samples are in Figure 1 as solid triangles). The samples were collected with a gasoline portable drill hole, water cooled, with diamond drill that cut cylindrical samples of 2.5 cm in diameter. The samples were oriented in the magnetic field using a leveled compass so magnetic azimuth and inclination angle could be determined. The volumetric magnetization was measured in a magnetometer of the Paleomagnetic Laboratory of Institute of Astronomy, Geophysics and Atmospheric Science of the Universidade de São Paulo (IAG-USP) and results in the sample referential system were them translated into local geographical sample.

Natural Remnant Magnetization (NRM) determinations include primary magnetization acquired at the time of rock formation and secondary magnetizations acquired after rock formation. It is important to remove the secondary magnetization to better determine the direction of the field at the time of the cooling of the alkaline intrusions. Two different techniques were applied to remove this information: (a) alternated magnetic field and (b) thermal demagnetization.

In the application of alternate magnetic field, the cycle begins with the induced magnetic field at the maximum intensity *H* and finishes at zero fields; at the end the existing magnetization is measured. When the induced magnetic field reaches *H* the magnetic moment of the grain whose coercivity is minor or equal to *H* will align at the same orientation of the applied magnetic field. When the field intensity goes to zero the magnetic grain loose its orientation and total magnetization will be equal to zero. There is a direct relationship between the intensity of the applied magnetic field and the mineral coercivity (Tauxe 2002).

In the case of demagnetization by thermal process it is possible to investigate the spectrum of blocking temperature (and its mineral composition) by heating the

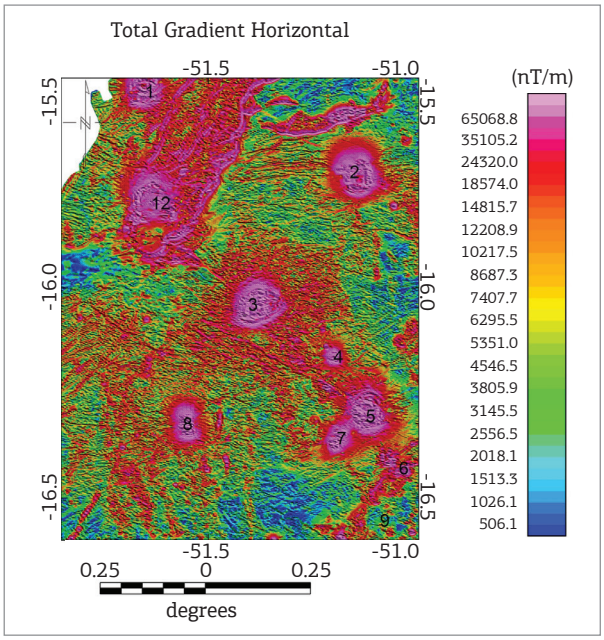

Figure 5. Map of the Total Horizontal Gradient (in color) and Analytical Phase Signal (in relief).

sample at monotonic increasing temperatures and measuring the magnetization after the cooling process for each step. The whole process — heating and cooling — is carried out in a zero magnetic field. The blocking temperature of each mineral is known and very stable until temperature is close to Curie point, so it is possible to determine the main magnetic minerals present at the sample and observe secondary magnetizations that are removed at lower temperature. After the rock is cooled only the MRN is present.

The remnant directions are calculated using the primary component. It is given the same weight to a point sequence that corresponds to an individual component. The direction of the characteristic remnant magnetization is calculated by least square method for the most stable directions measured.

The mean direction is calculated using Fisher's statistics (Fisher 1953). It considers all N vectors whose intensity is equal to one and the mean of directions $< \vec{S} >$ equal to the vectorial sum ($< \vec{R} >$) of the all N vectors divided by their intensity R ($< \vec{S} > = \vec{R} / R$). Fisher (1953) suggests some statistical parameters to define the data groups and reliability of the mean direction obtained. The precision parameter K defines the direction dispersion over a sphere of unitary radius. The best estimate for the value of K (for $N > 3$) is given by the relation: $K = [(N-1) / (N-R)]$. The obtained directions will be grouped if N is close to R (i.e. K has a high value). If the data dispersion is very high then R will be smaller than N and K parameter will have a low value. The angle $\alpha_{95} \approx 140^{o}/\sqrt{KN}$ is another parameter that may be considered. It represents twice the standard deviation using spherical projection.

The populations of MNR magnetizations directions that follow Fisher's density distribution function were isolated with the two demagnetization processes, alternate fields and thermal process. The analyzed samples showed multiple components that were very well defined in orthogonal directions. For the samples majority the less stable components were isolated between 0 – 20 mT on average (Fig. 6A). In the thermal demagnetization the less stable components were isolated between 0 and 600 °C on average (Fig. 6B). Those components were interpreted as secondary remnant magnetization acquired after rock cooling.

Figure 7 presents the magnetization direction (declination and inclination at the local geographic reference system) using stereographical projection. Two groups are defined in the figure. One composed by south direction and negative inclination represented by samples 01, 04, 07 and 10, located at most north area of the GAP. Figure 6 shows examples of demagnetization results of this component. The second group has direction pointing towards north with positive inclination. They were found at sites 06, 09A and 09B located at the central part of the GAP. It was not possible to complete isolate the primary remnant magnetization using alternate fields for samples from site 09. So, in a later step samples from this site were submitted to the thermal demagnetization. This process was also applied to a few specimen of each site.

The mean magnetization direction for each site was calculated using just the specimens that presented coherent magnetizations and acceptable statistical parameters (Fig. 7B), that is, sites 01, 04 and 07. Table 2 presents a summary with the mean direction and statistical parameter for each site. The mean values of susceptibility and magnetic direction were used in the reference models for the inversion procession of GAP aeromagnetic data.

3D INVERSION OF MAGNETIC DATA

The anomalous field produced by the distribution of magnetization $J = J_x J_y J_z$ is given by the following integral equation with a dyadic Green's function:

$$T(\vec{r}) = \frac{\mu_0}{4\pi} \int_V \nabla\nabla \frac{1}{|\vec{r} - \vec{r}'|} \cdot \vec{J} dv \qquad (1)$$

where $\mu_0 = 1$ is the magnetic permeability, $T(x_i, y_i, z_i)$ is the observation of the jth rectangular prism, and r is the position of the observation point. V represents the volume of magnetization (MAG3D 2002).

In 3D inversion the source and substrate are discretized into M cells, and each cell has uniform magnetization. The observations $T(x_i, y_i, z_i)$ are approximated by a continuous function, the integrals of equation (1), expressing

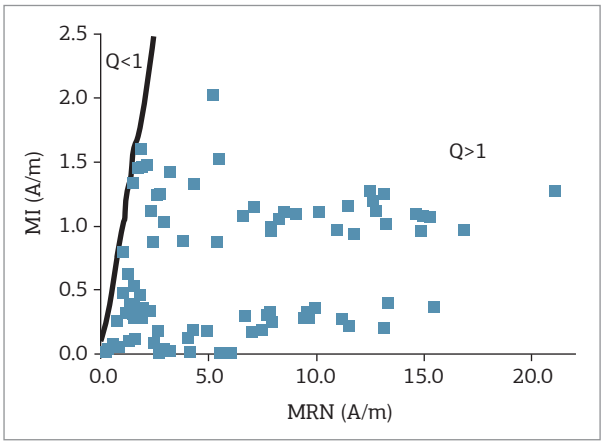

Figure 6. Remnant versus induced magnetization plot with the Konigsberger ratio (Q) equal 1 (solid line) separating fields for relative importance of remnant (Q > 1) and induced (Q < 1) magnetization on each sample.

the relationship between the physical property, magnetic susceptibility, and the corresponding magnetic observations. Some methods use a linear formulation for the inverse problem and, in this case, divide the subsurface into a set of prismatic cells with known size and position, but with contrasting physical property unknown. The interpretive model consist of 3D prisms juxtaposed with constant magnetic susceptibility into each prism to be determined. The distribution of magnetization in these blocks delineates the magnetic source in the region generating the total field anomaly observed, represented by equation (1).

Li and Oldenburg (1996) developed an inversion technique to determine the distribution of magnetic susceptibility. They considered that the model is directly proportional to the magnetic field anomaly and varies on a linear scale (software

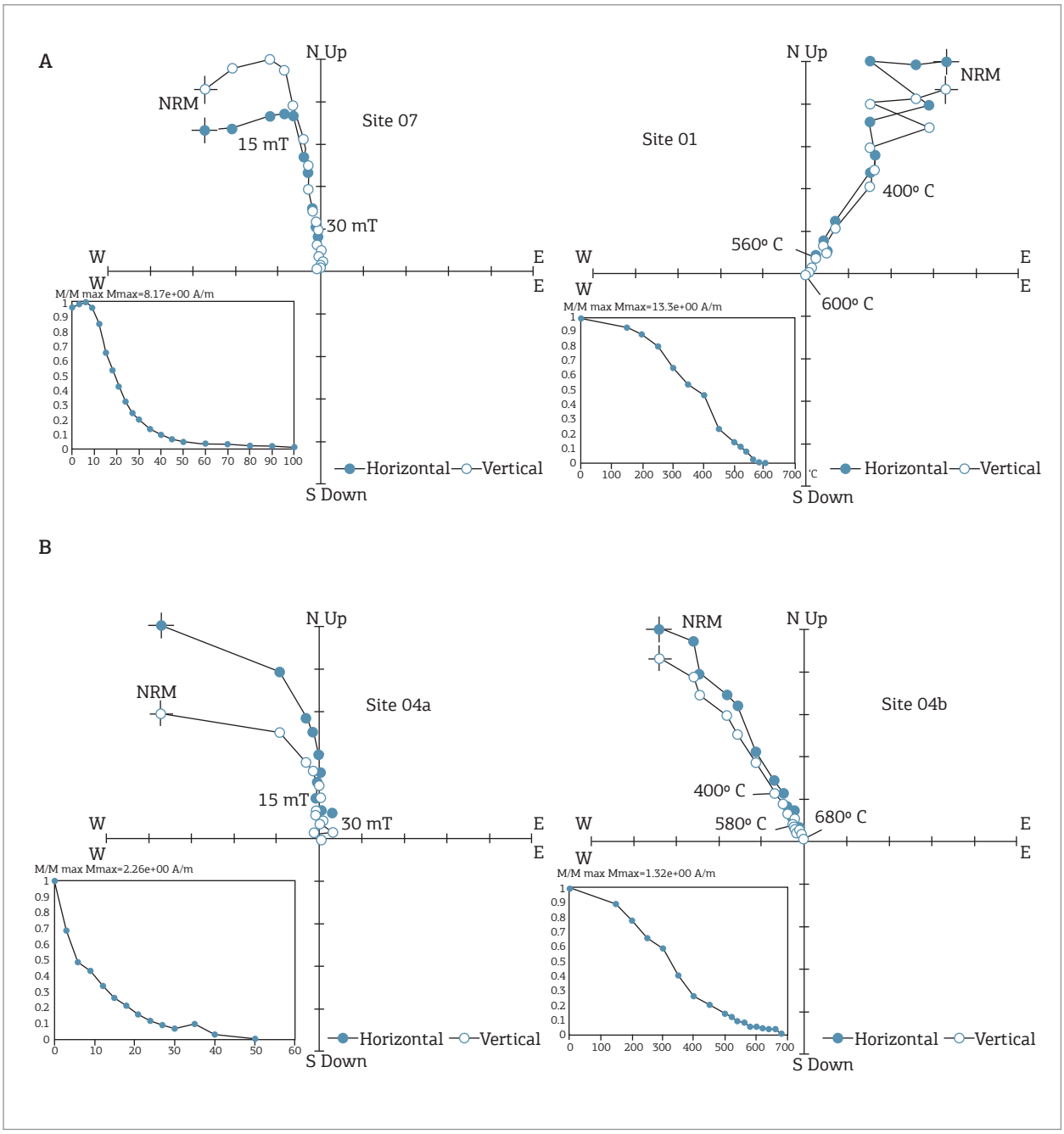

Figure 7. Example of the isolation of a magnetization component for one specimen. (A) Orthogonal projection (Zijderveld's diagram) of demagnetization by alternate fields with intensity curve normalized by the applied fields at it side. (B) Orthogonal projection (Zijderveld's diagram) of thermal demagnetization with intensity curve normalized by the temperature at its side.

Table 2. Mean magnetization direction, represented by the inclination (*I*) and declination (*D*), sample numbers for each site (*N*) and statistical parameters *R*, *K* and α_{95} (°), as described in the text.

Site	D (°)	I (°)	N	R	K	α_{95} (°)
01	23.00	-43.60	10	9.9	140.4	8.30
04	340.00	-32.80	8	7.9	155.4	5.70
07	356.00	-42.40	8	7.8	42.1	5.50
Mean	**1.8**	**-40.3**	--	--	--	**17.6**
06	88.40	27.00	6	5.9	36.5	9.60
09A	66.30	26.30	6	5.8	24.4	21.20
09B	61.10	36.50	8	7.7	25.3	10.80
10	83.00	-29.70	7	6.9	79.9	11.20
Mean	**72.2**	**30.5**	--	--	--	**21.2**

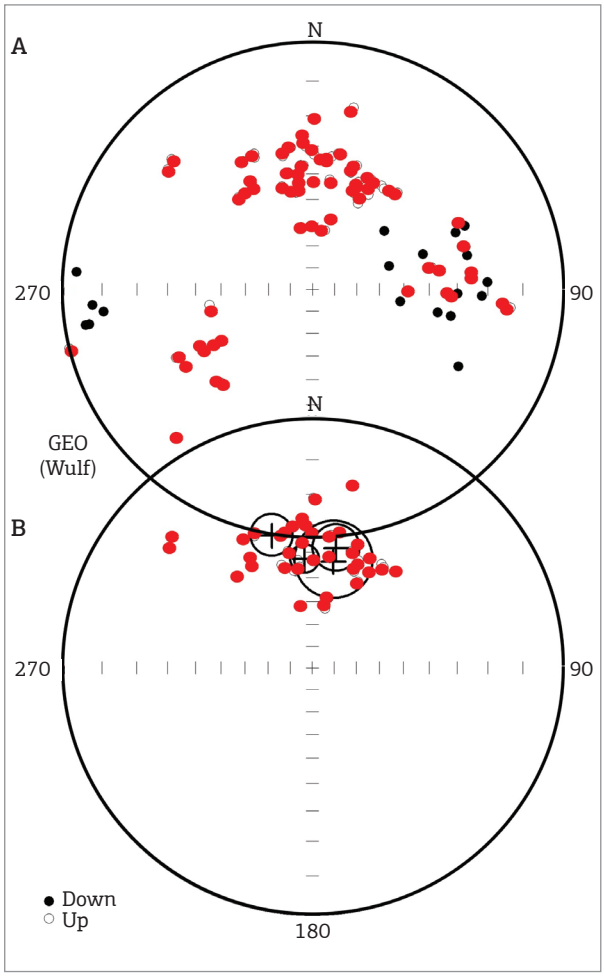

Figure 8. Stereographical projection of mean directions of all sites of GAP (A) and of the sites that presents coherent magnetizations directions with acceptable statistical parameters (sites 1, 4 and 7) (B). Open circles for upper hemisphere and solid circles for lower hemisphere.

MAG3D, 2002). The algorithm assumes that the source region is represented by a set of rectangular cells in a 3D orthogonal mesh with magnetic susceptibility (κ) constant in each cell. Since the number of cells is grater than the number of available data, as pointed out by Li and Oldenburg (1996), they proposed the introduction of an objective function that can incorporate a priori information, with appropriate weighting that is minimized and can produce a geological acceptable model. This objective function is described as (Li & Oldenburg 1996):

$$\phi_m(\vec{K},\vec{K_0}) = \alpha_s \int_V W_s (w(z)[\vec{K}-\vec{K_0}])^2 dV +$$
$$\alpha_x \int_V W_x \left(\frac{\partial w(z)[\vec{K}-\vec{K_0}]}{\partial x}\right)^2 dV +$$
$$\alpha_y \int_V W_y \left(\frac{\partial w(z)[\vec{K}-\vec{K_0}]}{\partial y}\right)^2 dV +$$
$$\alpha_z \int_V W_z \left(\frac{\partial w(z)[\vec{K}-\vec{K_0}]}{\partial z}\right)^2 dV \quad (2)$$

In the objective function of model the terms W_s, W_x, W_y e W_z are spatially dependent weighting functions and α_s, α_x, α_y and α_z are coefficients that affect the relative importance of different components in the objective function. The weight function $w(z)$ does not allow that magnetic susceptibility be concentrated near the surface. It is convenient to write Eq (2) as $\varphi_m(p) = \varphi_{ms} + \varphi_{mv}$ where φ_{ms} refers to the first term in Equation (2) and φ_{mv} refers collectively to the three remaining terms involving the variation of the model in the three spatial directions. The reference model can be included in φ_{ms} and if necessary, remove any remaining other terms.

Li and Oldenburg (1996) used a weight function w to prevent the rapid decay of magnetic surface data with depth in the resolution. If this fact is not controlled the magnetic susceptibility is concentrated near the surface. The weight function, $w(z) = (z-z_0)^{-\beta/2}$, is then applied into φ_{ms} and optionally into φ_{mv}, β is usually set equal to 3 and z_0 depends on the cell size of the model and the altitude of the observation data. The steps for discretization of the model are described in Li and Oldenburg (1996).

After the definition of the initial model, the program seeks a solution that minimizes φ_m, explain the data within an experimental accuracy (δ) and keep the magnetic susceptibility

values positives. This is achieved by minimizing $\varphi = \varphi_d + \lambda\varphi_m$ subject to $\kappa_j > 0$, as shown in Equation (3):

$$\varphi = \left\| W_d (d^{obs} - d^{calc}) \right\|^2 + \lambda \left\| W_m (\vec{K} - \vec{K}_0) \right\|^2 + 2\zeta \sum_{j=1}^{M} ln(K_j) \qquad (3)$$

where φ is the global objective function, λ is the regularization parameter and ζ is the barrier parameter for the maximum and minimum values of the magnetic susceptibility contrast. In Equation (3), λ controls the relative importance of the model norm and data fitting. The constraint of positivity is implemented in the logarithmic term of Equation (3) (Li & Oldenburg, 2003).

The presence of strong remnant magnetization can pose severe challenges to the quantitative interpretation of magnetic data. Problems stem from the fact that the direction of total magnetization is unknown and can be significantly different from that of the current inducing field. In applications such as crustal scale studies the remanence is often very strong and cannot be ignored. Inversion techniques require recovered causative bodies to reproduce the observed data, and this dictates that we must know the magnetization direction. Unrealistic distribution of magnetization and susceptibilities can result from inversion if incorrect direction is specified. Faced with this difficulty, one can take several different approaches. The first is to physically measure the remnant magnetization by oriented sample, with number of samples may necessarily give good characterization of the bulk magnetization direction. Once you have the knowledge of the direction of the remnant magnetization taken from oriented samples, we can use the total magnetization direction as the vector sum of the directions of magnetization induced more remaining.

We present a method for inverting surface magnetic data to recover 3-D susceptibility models. To allow the maximum flexibility for the model to represent geologically realistic structures, we discretize the 3-D model region into a set of rectangular cells, each having a constant susceptibility. The number of cells is generally far greater than the number of the data available, and thus we solve an underdetermined problem. Solutions are obtained by minimizing a global objective function composed of the model objective function and data misfit. The algorithm can incorporate a priori information into the model objective function by using one or more appropriate weighting functions. How the algorithm assumes that there is no remnant magnetization and that the magnetic data are produced by induced magnetization only, we can use the total magnetic intensity and direction of the total magnetization as the vector sum of the directions of magnetization induced more magnetization remnant.

RESULTS OF MAGNETIC INVERSION

The study area was divided into a set of cubic cells with 2 km side and constant value for the magnetic susceptibility. The initial model is composed of prisms centered in the anomaly positions outlined in Fig. 8, with the top at the surface, 0 km, and the base at 12 km depth.

The MAG3D inversion algorithm (MAG3D 2002) uses only induced magnetization, but the GAP alkaline intrusions have a strong remnant component as it was discussed previously. To overcome this situation it was used the direction of the total magnetization of the main alkaline sources. It was considered only the specimens that showed consistent magnetization directions to determine the average direction of the remnant magnetization so it was only considered sites 01, 04 and 07, as shown in Fig. 7B. The value obtained for the mean direction of remnant magnetization was I_R = -40.3º and D_R = 1.8º. The vector sum of the components of the induced magnetization M_I (magnetic field at the time of survey in the area has I = -19.5° and D = -18.5 °) and remnant magnetization M_R resulted in the direction of the total magnetization used in the inversion procedure, I_T = -39.0º and = D_T = 1.0 º.

Results from magnetic susceptibility measurements on the samples were set as the initial values of magnetic susceptibility (κ) in model, with κ varying according to values of Fig. 2. The values for the lateral extension of the intrusions were obtained by the analysis of the map of GHT and ASP (Fig. 8). Depth of the top was set at 0 km for the outcrops and 2 km for the two magnetic anomalies with no geological evidence on the surface. Geometrical parameters for the initial model are summarized in Table 3.

Figure 9 shows the modeled subsurface distribution of magnetic susceptibility from the inversion. In the inversion process the limit values for the physical parameters imposed on each prism are κ_{min} = 0.0 (SI) κ_{max} = 0.1 (SI). The distribution of magnetic susceptibility in depth occupies more

Table 3. Initial parameters for the reference model in the 3D magnetic inversion.

Alkaline Intrusion	Extension (km)[a]	Top depth (km)
1- Morro do Engenho	8.0	0.1
3- Montes Claros de Goiás	10.0	0.1
12- Registro do Araguaia	10.0	2.0
13- Anomaly 2	6.0	2.0
3- Montes Claros de Goiás	10.0	0.1
4- Diorama	4.0	0.1
5- Córrego dos Bois	8.0	0.1
7- Buriti	4.0	0.1
2- Santa Fé	6.0	0.1

[a]X and Y extension have the same value.

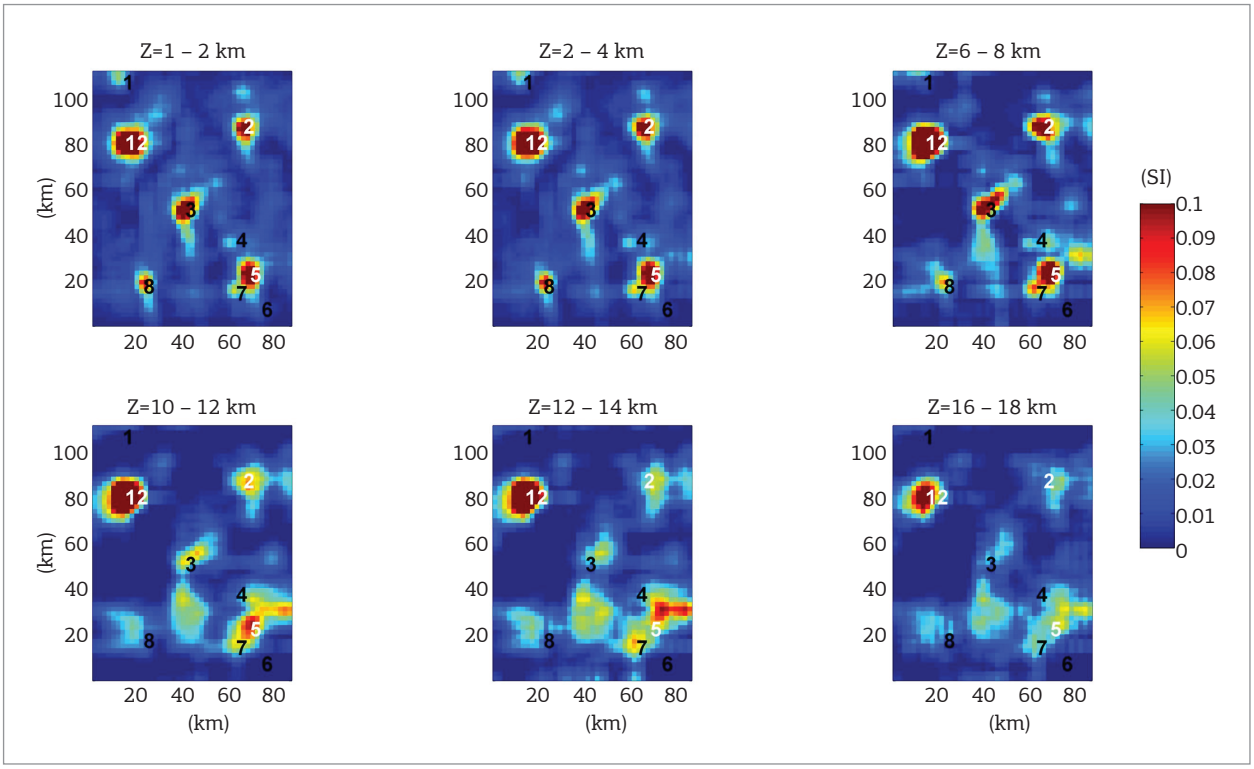

Figure 9. Magnetic susceptibility distribution in depth from the 3D inversion. Slices cut at different depths.

cells in x and y directions than the reference model used. For most of the GAP intrusions the depth was around 10 – 12 km, except Registro do Araguaia with magnetic susceptibility at depths up to 16 km. The possible intrusion that corresponds to this anomaly (n. 12) does not outcrop. Its top depth was estimated by Dutra *et al.* (2012) from the Euler deconvolution method combined with analytical signal amplitude applied to the magnetic anomaly reduced to the pole. Dutra *et al.* (2012) found the top at a depth around 600 – 800 meters. Figure 9 shows slices of magnetic susceptibility variation at depths varying from 2 to 16 km. The subsurface distribution is not homogeneous with depth; most of the intrusion has more area with physical property contrast at 6 – 8 km depth. Another feature is the dispersion of susceptibility at depth in the south part the area, especially at the depth of 12 – 14 km, suggesting a smooth connection among them. This distribution allows a hypothesis of some intrusions with more spherical shapes than cylinder, as could be expected for alkaline intrusions that usually resembles pipe structures.

From the distribution model (Fig. 9) it was calculated the magnetic field by forward modeling and its result was compared with the observations as can be seen in Fig. 10. The modeled magnetic amplitude fits the data, but the magnetic field (red line) is smoother compared with observation (black line).

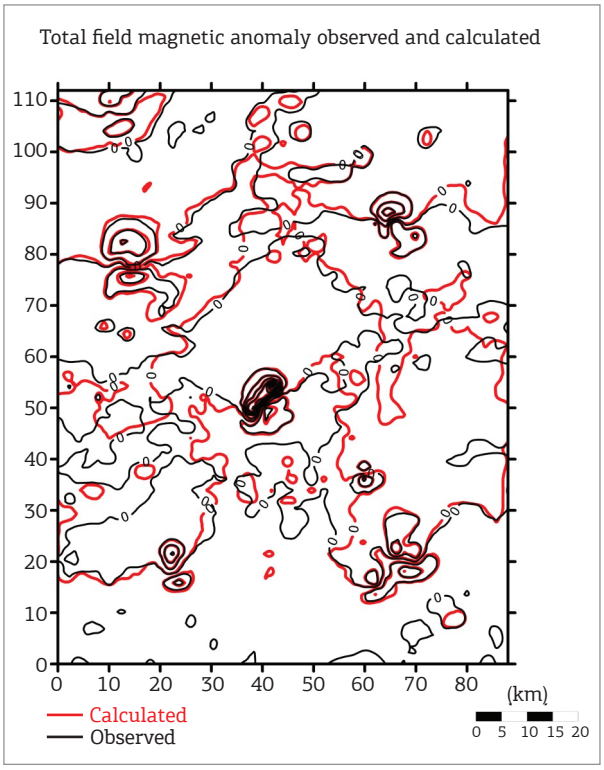

Figure 10. Total field magnetic anomaly (black line) and magnetic anomaly calculated from the inversion magnetic susceptibility distribution (red line).

This smoothing results from the limited number of cells that the program allows and combined with the choice of inverting all the area together instead of different groups of anomalies. This choice reflects the main focus of this work that is to understand the emplacement of the intrusions within the crust, which resulted in the maximum possible number of cells with a larger size.

The results in Fig. 10 represent the contribution of the magnetic field produced by the remnant magnetization more induced magnetization used as the "induced magnetic field" as a work hypothesis. This is not the strict way for the MAG3D inversion algorithm but the good fit between observation and model indicates that the chosen way worked adequately.

DISCUSSION AND CONCLUSIONS

The aeromagnetic signal of the alkaline intrusions of the GAP was used to obtain the magnetic susceptibility distribution in subsurface and the model may represent the distribution of magnetic mineral content. The authors knew from previous work (Dutra & Marangoni 2009) that the magnetic signal observed in the area is a combination of induced and remnant magnetic components. The difficult to invert a source with remnant magnetism is great and this resulted in a search for a different path using known algorithm. The path chosen was to use the sum vector of the components as the induced field in the area. To accomplish this procedure a careful analysis of remnant component was done.

The main component of remnant magnetization was isolated using alternate magnetic field and thermal demagnetization. The results considering just the most stable samples and with acceptable statistical parameters, sites 01, 04 and 07 as is seen in Table 2, resulted in remnant inclination and declination of -40.3º and 1.8º, respectively. These values were summed with the induced field at the flight time to provide values for the inversion algorithm. Measurements of magnetic susceptibility and density also provided values for physical parameter in the inversion.

To complete the initial model the geometry of the sources was preliminary find with the application of Total Horizontal Gradient and Analytical Signal Phase on the total anomaly field reduced to the pole. The superimposed map with the two results (Fig. 8) marks the contact limits and also some NW-SE faults that cross the anomalies without changing their shape. This may suggest that this faults or lineaments were weakness regions and the alkaline magma may take advantage of it during the emplacement. The NE-SW lineaments in the north of Registro do Araguaia (anomaly 12 in Fig. 8) may be a different case. We propose that this anomaly is located at the southern end of the Transbrasiliano Lineament and that the magma emplacement filled the fractures of the lineament. We also propose that Registro do Araguaia and its NE-SW lineament may be the main locus for magma conduit based on the anomaly size, strong magnetic expression and source size from inversion. The two main direction observed in Fig. 8 were reactivated as extensional tectonics during magma ascent. The NW-SE lineament, with traces in the magnetic maps, was very active and in this direction it is possible to find other alkaline provinces, the Alto Paranaíba Province (APIP), at the SE of the area and Poxoreu Province at the NW of the area. A discussion of the importance of this lineament can be found in Marangoni and Mantovani (2013).

The results from the 3D inversion indicate that the intrusions extents through the upper crust, from surface up to 10 – 12 km. The results suggest that the shapes of the bodies are conical. Except for the Registro do Araguaia shows differences respecting the other intrusions. Its depth goes up to 16 km and the area involved is also bigger than the rest of the intrusions. It is reasonable to consider that Registro do Araguaia is one of the most important magma feeder for the GAP intrusions. By the 3D inversion, the magnetic susceptibility is distributed in almost spherical and cylindrical shapes. The possibility of spherical shapes arise the hypothesis that the GAP intrusions at the north part of the province represent magmatic chambers. The alkaline magma ascend from the lithosphere, used the two main fault systems as space for emplacement. Results from magnetic inversion confirm the conclusions from Junqueira-Brod *et al.* (2005) and Dutra *et al.* (2012).

If we combine the results from Figs. 8 and 9 it is possible to consider that the north region of the GAP show two different configurations: one of big anomalies and susceptibility distribution at the most north of the area, including important linear features maybe related with the Transbrasiliano Lineament and predominantly aligned at the NE-SW direction. The south part of the area has smaller intrusions, crossed by magnetic lineaments at the NW-SE direction, that could be related with the 125 Az Lineament, the same one where other two provinces took place. Chemical analysis confirmed the alkaline and subalkaline character of the magmas. The high MgO content shows the primitive character of these intrusions, the Ba anomaly is a characteristic of intracontinental magmatism and can be attributed to the phlogopite presence in the mantle source or crustal contamination. According to Carlson *et al.* (2007) the Goiás mafic–alkalic magmatism is the result of remelting of Brasiliano belt lithospheric mantle composed of peridotite veined with the crystallization products of infiltrating Mesoproterozoic melts. Since this mixed lithospheric mantle also would have

isotopic compositions similar to the Paraná flood basalts, the results presented here suggest that the Paraná high-Ti source, and that of the isotopically similar oceanic basalts of the Walvis Ridge, formed in the Brazilian lithosphere in the Proterozoic.

Acknowledgments

This work was supported by Fundação de Amparo à Pesquisa do Estado de São Paulo – FAPESP, 2006/00201-2 and 2007/53179-7. The authors acknowledge M. B. Lacerda for density measurements.

REFERENCES

Blakely R.S. 1996. Potential theory in gravity and magnetic applications. Cambridge, Cambridge University Press.

Books G.K. 1962. Remanent magnetization as a contributor to some aeromagnetic anomalies. *Geophysics*, **27**(3):359-75.

Brod J.A., Barbosa E.S.R., Junqueira-Brod T.C., Gaspar J.C., Diniz-Pinto H.S., Sgarbi P.B.A., *et al.* 2005. The Late Cretaceous Goiás alkaline Province (GAP)m Central Brazil. *In*: Comin-Chiaramonti, P. & Gomes, C.B. (eds.). Mesozoic to Cenozoic alkaline magmatism in the Brazilian platform. São Paulo; EDUSP-FAPESP. pp. 261-416.

Carlson R.W., Araujo A.L.N., Junqueira-Brod T. C., Gaspar J.C., Brod J.A., Petrinovic I.A., *et al.* 2007. Chemical and isotopic relationships between peridotite xenoliths and mafic– ultrapotassic rocks from Southern Brazil. *Chemical Geology*, **242**(3-4):415-34.

Comin-Chiaramonti P. & Gomes C.B. (eds). 2005. Mesozoic to Cenozoic alkaline magmatism in the Brazilian platform. São Paulo; EDUSP-FAPESP, 752p.

Cox K.G., Bell J.D., Pankhurst R.J. 1979. The interpretation of igneous rocks. G. London; Allen & Unwin.

Dutra A.C., Marangoni Y.R. 2009. Gravity and magnetic 3-D inversion of Morro do Engenho complex, central Brazil. *Journal of South American Earth Sciences*, **28**(2):193-203.

Dutra A.C., Marangoni Y.R., Junqueira-Brod T.C. 2012. Investigation of the Goiás Alkaline Province, Central Brazil: Application of gravity and magnetic methods. *Journal of South American Earth Sciences*, **33**(1):43-55.

Fisher R. 1953. Dispersion on a sphere. *Proceedings of the Royal Society of London - Series A*, **217**:295-305.

Junqueira-Brod T.C., Riog H.L., Gaspar J.C., Broad J.A., Meneses P.R. 2002. A Província Alcalina de Goiás e a extensão de seu vulcanismo kamafugítico. *Revista Brasileira de Geociências*, **32**(4):559-66.

Junqueira-Brod T.C., Gaspar J.C., Brod J.A., Jost H., Barbosa E.S.R., Kafino C.V. 2005. Emplacement of kamafugite lavas from the Goiás Alkaline Province, Brazil: constraints from whole-rock simulations. *Journal of South American Earth Sciences*, **18**(3-4):323-35.

Lacerda Filho J.V., Rezende A., Silva A. 2000. Programa Levantamentos Geológicos Básicos do Brasi. Geologia e Recursos Minerais do Estado de Goiásb e do Distrito Federal. Escala 1:500000 (mapa) 2ª Edição. CPRM/METAGO/UnB. 184 pp.

LASA Engenharia e Prospecções S.A. 2004. Projeto Levantamento Aerogeofísico do Estado de Goiás – 1ªEtapa – Arco Magmático de Arenópolis – Complexo Anápolis - Itauçu – Sequência Vulcano-Sedimentar de Juscelândia. Relatório Final do Levantamento e Processamento dos Dados Magnetométricos e Gamaespectrométricos, Convênio de Cooperação Técnica entre a SGM/MME/CPRM e SIC/SGM/FUNMINERAL/Estado de Goiás, Relatório Final, 22 vol., Texto e Anexos (mapas), Rio de Janeiro.

Le Bas M.J., Le Maitre R.W., Streckeisen A. Zanettin B. 1986. A chemical classification of volcanic rocks based on the total alkali-silica diagram. *Journal of Petrology*, **27**(3):745-750.

Le Maitre R.W. 1989. A classification of igneous rocks and glossary of terms. Oxford: Blackwell Scientific Publications. 193p.

Li Y., Oldenburg D.W. 2003. Fast inversion of large-scale magnetic data using wavelet transforms and a logarithmic barrier method. *Geophysics Journal International*, **152**(2):251-65.

Li Y., Oldenburg D.W. 1996. 3D inversion of magnetic data. *Geophysics*, **61**(2):394-408.

MAG3D. 2002. A program library for forward modeling and inversion of magnetic data over 3D structures, version 3.1, Department of Earth and Ocean Sciences. Vancouver; University British Columbia.

Marangoni Y.R., Mantovani M.S.M. 2013. Geophysical signature of alkaline intrusions bordering the Paraná Basin. *Journal of South American Earth Science*, **41**:83-98.

Reid A.B. 1980. Aeromagnetic survey design. *Geophysics*. **45**(5):973-6.

Roest W. R., Pilkington M. 1993. Identifying remnant magnetization effects in magnetic data. *Geophysics*, **58**(5):653-9.

Sgarbi P.B.A., Clayton R.N., Toshiko KM., Gaspar J.C. 1998. Oxygen isotope thermometry of Brazilian potassic volcanic rocks of kamafugitic affinities. *Chemical Geology*, **146**(3):115-26.

Tauxe L. 2002. Paleomagnetic principles and pratice. Kluwer Academic Publishers, Dordrecht.

Telford W.M., Geldart L.P., Sheriff R.E. 1990. Applied Geophysics. New York, Cambridge University Press.

Arquivo digital disponível on-line no site www.sbgeo.org.br